

Document Version

Final published version

Licence

CC BY

Citation (APA)

Ghosh, A., & Haverkort, J. W. (2026). Modulating the current in water electrolysis does not increase energy efficiency compared to a constant equal average current. *International Journal of Hydrogen Energy*, 221, Article 154195. <https://doi.org/10.1016/j.ijhydene.2026.154195>

Important note

To cite this publication, please use the final published version (if applicable). Please check the document version above.

Copyright

In case the licence states "Dutch Copyright Act (Article 25fa)", this publication was made available Green Open Access via the TU Delft Institutional Repository pursuant to Dutch Copyright Act (Article 25fa, the Taverne amendment). This provision does not affect copyright ownership.

Unless copyright is transferred by contract or statute, it remains with the copyright holder.

Sharing and reuse

Other than for strictly personal use, it is not permitted to download, forward or distribute the text or part of it, without the consent of the author(s) and/or copyright holder(s), unless the work is under an open content license such as Creative Commons.

Takedown policy

Please contact us and provide details if you believe this document breaches copyrights. We will remove access to the work immediately and investigate your claim.



Modulating the current in water electrolysis does not increase energy efficiency compared to a constant equal average current

Anamika Ghosh ^{*} , J.W. Haverkort 

Process and Energy Department, Delft University of Technology, the Netherlands

ARTICLE INFO

Keywords:

Anion exchange membrane
Pulse electrolysis
H₂ production
Energy consumption

ABSTRACT

Modulating the potential or current amplitude can improve mass transfer and assist in the bubble removal of electrochemical processes. However, the impact on energy efficiency of water electrolysis requires careful assessment. This study examines an anion exchange membrane (AEM) electrolyser under pulsed and direct current (DC) operating conditions. Two cathode catalysts were tested using square pulses with a duty ratio of 0.5 and 0.9 across 0.005–500 Hz. The pulsed method consumes more or comparable energy compared to the DC case at a time-averaged current density of 295 mA/cm² in 1 M KOH. Unlike most studies, we argue that a fair comparison can only be made at an equal average current density to ensure same hydrogen production rate. Using this metric, we find no evidence of any improvement under the tested conditions, highlighting the need for a more rigorous evaluation of the effectiveness of dynamic power strategies.

1. Introduction

Hydrogen (H₂) is a promising clean fuel in the global transition to net-zero emissions. Among various production methods, alkaline water electrolysis is a proven and potentially cost-effective method. Although it is one of the oldest techniques, it still faces challenges in becoming commercially attractive compared to the CO₂-emitting alternative of steam methane reformation (SMR). Recent reports suggest that the estimated cost of green H₂ ranges from USD 4–9/kg versus USD 1.5–2/kg for SMR. As a result, several strategies have been explored to address the efficiency and cost challenges of water electrolyzers.

Among these, pulsed electrolysis has gained significant attention over the past decade because of its potential to improve mass transfer, bubble removal, and reaction kinetics. Voltage- or current-modulation has been investigated for electrodeposition [1], the oxygen reduction reaction (ORR) [2], CO₂ electrolysis [3], and also water electrolysis [4]. However, despite its early origins [5,6], the advantage of pulsed methods for water electrolysis is not well understood. Although recent reviews [7–10] have summarised the advances of pulse electrolysis in general; here we focus exclusively on its application to water electrolysis. We note that, instead of pulsed operation, sometimes the synonymous term ‘forced periodic operation’ is used [11,12], especially in the chemical engineering field.

Historically, foundational studies (pre-2000) focused on under-

standing the fundamental electrochemical behaviour under voltage or current pulses. For instance, Tseung et al. [5] studied H₂ evolution (HER) at platinum electrodes using potentiostatic pulses to monitor microstructure-dependent kinetic behaviour under short operational durations. Similarly, Bockris et al. [6] applied a potentiostatic pulse to a homopolar generator to produce H₂ and observed nearly double the current compared to steady-state conditions. Hitz and Lasia [13] later explored HER kinetics on platinum electrodes using galvanostatic pulses. However, the influence of pulses was not explicitly explained in these studies.

Between 2000 and 2015, comparative studies between pulsed and DC methods gained momentum. Shimizu et al. [14] found that for almost all tested conditions, DC electrolysis produced more hydrogen at equal power consumption, only for a 7.9 V, 1.2 A, 17 kHz inductive pulse a small improvement was found, which remains to be verified. Mazloomi et al. reported a 15 % reduction in power consumption using pulsed electrolysis at resonant frequencies where the observed current is maximum [15]. However, the use of aluminium electrodes in KOH solution raises concerns regarding dissolution. Furthermore, this study lacked detailed information on the applied pulse characteristics and power calculations. Huang [16] observed that pulsed electrolysis could achieve the same H₂ production rate with half the energy consumption compared at a current density of 180 mA/cm² to DC electrolysis. Similarly, Lin et al. [17] demonstrated an 88 % reduction in power

^{*} Corresponding author.

E-mail addresses: anamikaghosh@tudelft.nl (A. Ghosh), J.W.Haverkort@tudelft.nl (J.W. Haverkort).

consumption using a 10 % duty cycle and 10 ms pulse ‘on’ time (t_{on}). However, their calculation did not account for the produced hydrogen volume under such a low-duty cycle, which predominantly keeps the electrolyser in the ‘off’ state.

Between 2016 and 2024, pulse electrolysis research advanced considerably. Dobo et al. [18,19] applied pulsed potentials to an alkaline water electrolyser (AWE) but noted the positive effect only when the base potential was below 1.8 V at low frequencies, where H_2 production was minimal. Vincent et al. [20] achieved reduced cell voltage using pulsed currents; however, their performance was benchmarked against values in the literature. De Radigues et al. [21] observed a current enhancement with a 2 ms pulse applied to a 3D Ni electrode, and Rocha et al. [22] showed a 17 % reduction in cell voltage with a 50 % duty cycle and a 28 % reduction with a 20 % duty cycle, respectively. However, these studies used the average voltage as a metric without keeping the hydrogen production rate equal. In a very interesting recent work, Cheng et al. [4] applied pulsed current to a 10 kW industrial AWE stack operating at 80°C and 10 bar. They showed an advantage of pulsed electrolysis at low load conditions by minimising the shunt currents. Erelil et al. [23] observed reduced energy consumption in a proton exchange membrane electrolyser (PEMWE) with pulse electrolysis. Zhang et al. [24] recently demonstrated a 27 % enhancement in H_2 production rate with a 28 % reduction in energy consumption at $f = 0.5$ Hz and $D = 0.5$. However, neither Erelil et al. nor Zhang et al. conducted a fair comparison of pulsed and DC electrolysis efficiency while keeping the total H_2 production constant.

Despite these advances, several methodological inconsistencies persist in the literature. Many studies mentioned above [16,21,22,24] inadequately compare the on-state parameters in the pulsed electrolysis with the steady-state values of DC over unequal time frames. Often, these authors did not adjust peak or base voltage to sustain the same average current or voltage as of DC. For example, Rocha et al. [22] compared the DC and pulse current performance at 0.3 A. However, in every current pulse, they varied the on/off time, keeping the peak and base voltage constant. Consequently, the average applied current in the pulsed method was 0.15 A, given $D = 0.5$, while for DC, it was 0.3 A. As the average current was low in pulsation, it led to a lower cell voltage than the DC. Such comparisons led to incorrect assessments of the efficiency of the pulsed method. A recent article by Zhang et al. [25] claimed an energy savings of 54.43 % due to reduced bubble coverage on the electrode surface. However, in this study, the applied voltage during the DC process was 8 V, while in the pulsed process, it was 4 V. The lower cell voltage resulted in a lower current, which naturally produced fewer gas bubbles. Therefore, the observed advantage in the pulsed method was not due to reduced bubble coverage, but rather an inconsistent application of voltages between the two methods. In many cases [21–24,26] the authors ignored the negative current during the ‘off’ time, where the base voltage was zero. The negative current can lead to a potential electrode polarity reversal. This highlights the significance of the choice of base voltage/current and maintaining the same average current density for a fair comparison of the DC and pulsed method efficiency.

Rarely is the power consumption of pulsed electrolysis compared to DC at equal average current density. An exception is the recent work of Cheng et al. [4], where an improvement was found at low loads. The reason is that in stacks at low loads, the efficiency is lowered due to the presence of shunt currents. Intermittently increasing the current gives relatively less shunt current than DC at a lower load. This is a very interesting observation that only gives benefits in bipolar stacks with an energy efficiency that increases non-monotonously with current density. The advantages and limitations of these studies are summarised in Table 1.

In literature, the positive effects of a pulsed potential/current on water electrolysers are attributed to a) Electrical double layer (EDL) perturbation and (b) pulsating diffusion layer, which allows faster ion transport during ‘on’ time and replenishment of ions during ‘off’ time.

Table 1

A summary of the literature that compares the reported performance of pulsed water electrolysis with DC. It is noted that improvements are almost exclusively reported for $j_{av} \neq j_{DC}$. Most often, when we could assess this quantitatively, we found that $j_{av} < j_{DC}$. In the rare cases that $j_{av} = j_{DC}$, higher power consumption is reported, except for Ref. [4], which applies only to stacks at low loads. A star (*) indicates that negative ‘reverse currents’ were observed during the voltage ‘off’ phase or polarity reversal in the case of current pulses. The double star (**) indicates that the study didn’t mention or show any clear applied voltage profiles to determine whether $j_{av} = j_{DC}$ or not. The triple stars (***) indicate that the study didn’t directly compare with DC but instead reported efficiency losses at different conditions, such as varying DC offset values, AC amplitudes, and frequency.

Year	Type	Comparison vs DC	Current	Ref.
1993	PEM	higher power for 25 kHz, $D = 0.01$ current pulses (*)	$j_{av} = j_{DC}$	[34]
2006	AWE	higher power consumption at 300 ns voltage pulse	$j_{av} < j_{DC}$	[14]
2012	AWE	15 % lower power for $D = 0.05$ voltage pulses (**)	Not clear	[15]
2013	PEM	lower power for $D = 0.5$, 50 Hz current pulses	$j_{av} < j_{DC}$	[16]
2016	AWE	20 % efficiency loss, $f = 5$ kHz & amplitude 0.1 V (***)	$j_{av} = j_{DC}$	[19]
2018	AWE	higher electrical power loss during current pulses	$j_{av} = j_{DC}$	[35]
2018	AWE	20-25 % less power for 1200 kHz $D = 0.5$ voltage pulses	$j_{av} < j_{DC}$	[29]
2019	AEM	5x higher j for $f = 250$ Hz $D = 0.5$ ($V_{DC} \neq V_{av}$) (*)	$j_{av} \neq j_{DC}$	[21]
2021	AEM	lower voltage for $f = 500$ Hz $D = 0.02$ (*)	$j_{av} < j_{DC}$	[7]
2024	AWE	18 % higher current at 10 kHz $D = 0.5$ ($V_{DC} \neq V_{av}$)	$j_{av} \neq j_{DC}$	[36]
2024	AWE	17 % higher efficiency in stack at low load	$j_{av} = j_{DC}$	[4]
2024	PEM	lower power consumption for 1-20 kHz $D = 0.5-0.8$	$j_{av} < j_{DC}$	[23]
2024	PEM	321 % higher current at 0.2 Hz $D = 0.5$, ($V_{DC} \neq V_{av}$) (*)	$j_{av} \neq j_{DC}$	[24]
2025	PEM	27 % higher current for $f = 0.0125-0.5$ Hz, $D = 0.5$, ($V_{DC} \neq V_{av}$) (*)	$j_{av} \neq j_{DC}$	[26]
2025	AWE	54.43 % lower energy for $f = 600$ kHz, $D = 0.5$ (*)	$j_{av} < j_{DC}$	[25]

The EDL at the electrode/electrolyte interface influences the local electric field and ion concentrations. Therefore, the pulse on/off time is indeed critical to ensure that the process does not become overly capacitive relative to the faradaic process due to incomplete charging or discharging. Such a situation would reduce electrolysis efficiency and H_2 production. If the Faradaic process dominates, the pulse and DC should demonstrate the same H_2 production efficiency at equal average current density, or else the pulsed method is only likely to be affected by the EDL layer during fast pulsing, leading to lower efficiency compared to DC. On the other hand, water electrolysis might not suffer diffusion-related limitations as other mass transport-limited reactions, such as electrodeposition, ORR, etc. For example, in pulse plating, pulsing plays a significant role in modulating the diffusion layer and thus allows faster diffusion of ions from the bulk. Wei et al. [27] showed that during water electrolysis, unlike electrodeposition or plating, ions did not need to move from the bulk but rather by the nearest H_2O molecule following the Grotthuss mechanism. Hence, H_2O is the primary reactant for water electrolysis, especially for HER, and the electrolysis process does not encounter mass transport limitations like electrodeposition. While mass transport limitations could arise at high current densities, that could be eliminated using continuous circulation of electrolytes.

We are not the first to raise questions concerning the various metrics used in the literature. Ref. [7] mentions that “the power should be calculated as the integral of the product of voltage multiplied by the current during the entire pulse period”. Puranen et al. [28] made this the topic of their paper in the context of dynamic operation and current ripple.

This study addresses these gaps by systematically evaluating the

performance of pulsed and DC methods on AEM electrolyzers. We propose to use as the primary metric the energy efficiency or specific energy consumption relative to DC at equal average current density as the primary metric. This work thoroughly compares energy efficiency under various pulse conditions, identifying critical limitations of pulsed electrolysis while establishing accurate evaluation criteria.

2. Theory

2.1. Current density

To support our claim, to be substantiated experimentally in section 4, that usually no improvement in energy consumption is expected from pulsed potentials, we first provide a simplified mathematical analysis here. Our main criticism of most of the studies in the literature is that, if they compared with DC at all, this comparison is usually between different average current densities

$$j_{av} = \frac{1}{T} \int_0^T j dt \quad (1)$$

Here, the time T over which is averaged is either the time of the experiment or, in the case of a repeating pattern, the used period. Periodically switching off or lowering the current density may improve the average potential or even the energy required per amount of hydrogen produced, but it also lowers the average current density. For a fair comparison, the same average amount of hydrogen per unit of time should be produced over time. This implies that the maximum current used should be higher than the average of the DC current to give the same average current density. However, a periodic increase in current density above the average usually more than offsets any potential advantage during phases of lower or zero current density. The reason is that, normally, due to ohmic and activation losses, energy efficiency is an increasing function of current density. Therefore, the periods of higher-than-average current density decrease the energy efficiency more than can be made up for during periods of lower-than-average current density.

2.2. Energy metrics

Mathematically, the time-averaged consumed power per unit area A , or *power density*:

$$\frac{P_{av}}{A} = \frac{1}{T} \int_0^T jV dt \quad (2)$$

with V the cell voltage. The maximum power that can be obtained from the higher heating value of hydrogen is $\frac{1}{T} \int_0^T jV_{tn} dt$ with $V_{tn} \approx 1.48$ V is the thermoneutral voltage. Therefore, we can define the ratio of these two power densities as the *energy efficiency*:

$$\varphi = FE \frac{j_{av} V_{tn}}{\frac{1}{T} \int_0^T jV dt} \quad (3)$$

Here, FE is the Faradaic efficiency or current efficiency: the fraction of the average current density that contributes to hydrogen production. It is immediately clear from Eq. (3) that, when the cell voltage V is an increasing function of j , the energy efficiency φ is minimised for $j = j_{av}$. Any other choice would require periods of higher j during which the increase in jV will be larger than the decrease in jV during periods of lower j .

Instead of energy efficiency, we can also look at the *specific energy consumption*:

$$SEC = FE \frac{\frac{1}{T} \int_0^T jV dt}{M j_{av} / 2F} \quad (4)$$

This is the amount of energy required per mass of hydrogen produced. Here, $M = 2.01568 \cdot 10^{-3}$ kg/mol is the molar weight of H_2 and $F = 96485.3321$ C/mol is Faraday's constant, so that $M/2F = 1.04455 \cdot 10^{-8}$ kg/C. In general, the right-hand side of Eq. (4) contains a multiplication by the Faradaic efficiency, in case part of the current does not go towards hydrogen generation.

In this study, we are mostly interested in comparing with direct current. Therefore, we define the *relative specific energy consumption*:

$$\frac{SEC}{SEC_{DC}} = \frac{FE}{FE_{DC}} \frac{\frac{1}{T} \int_0^T jV dt}{j_{av} V_{DC}} = \frac{\varphi_{DC}}{\varphi} \quad (5)$$

which, by Eq. (5), is the inverse of the relative energy efficiency.

Let us consider an illustrative example. Consider the simplest cell model that only includes resistance, so $V = ARj$ and a Faradaic efficiency of FE = 100 %. In this case, Eq. (5) can be read as an integral form of the Cauchy-Schwarz inequality: $\frac{SEC}{SEC_{DC}} = \frac{1}{T j_{av}} \int j^2 dt \geq 1$. This inequality can be proven rigorously mathematically. It illustrates how, generally, voltage losses that increase with increasing current density will prefer DC over pulsed potential when it comes to minimising specific energy consumption at equal average current density.

For later reference, we here define the duty cycle of a square-wave current pulse consisting of a repeated cycle of a high current density for a time t_{high} followed by a lower current density for a time t_{low} as

$$D = \frac{t_{high}}{t_{high} + t_{low}} \quad (6)$$

This is usually defined for a cycle in which the lower current density is zero, so that the current is 'off'. However, here we also use it to represent the more general case of a nonzero lower current. This quantity is alternatively referred to as the power cycle, duty factor, or duty ratio. To fully define our cycle, besides the frequency f and duty cycle D , we also have to specify, for example, the high current density j_{high} and the low current density j_{low} , or alternatively the average current density $j_{av} = D j_{high} + (1 - D) j_{low}$. Equation (5) becomes in this case

$$\frac{SEC}{SEC_{DC}} = \frac{FE}{FE_{DC}} \frac{D j_{high} V_{high} + (1 - D) j_{low} V_{low}}{j_{av} V_{DC}} \quad (7)$$

where V_{high} and V_{low} are the voltages associated with j_{high} and j_{low} , respectively. In the case of a simple offset-resistance polarisation model $V = V_0 + ARj$ and with FE = FE_{DC} this becomes after some algebra

$$\frac{SEC}{SEC_{DC}} = 1 + \frac{(1 - D) D (j_{high} - j_{low})^2}{j_{av} (V_0 / AR + j_{av})} \quad (8)$$

Also, from this expression, it is clear that the SEC cannot be lower than in DC.

2.3. Literature gap

Why do we stress the importance of comparing pulsed potentials at equal hydrogen production rate, or in the case of 100 % Faradaic efficiency towards hydrogen, the average current density? This is because it is easy to report improvements in energy efficiency at a lowered current density precisely because the cell voltage usually decreases with decreasing current density. However, we do not need pulsed potentials for this: we can simply lower the average current density. However, this is usually not preferred since a high average current density is desirable for economic reasons, as the amount of hydrogen produced is directly proportional to the current density.

Stated in this way, it is not surprising that when scrutinising the literature, hardly any results of an improvement over DC, at equal average current density, can be found. An exception is the recent paper by Cheng et al. [4], where increased energy efficiency was reported at low current densities upon pulsing. The reason is that these experiments

were performed in several cells in series in a stack, allowing shunt currents to appear. In this phenomenon, the ionic current skips one or more cells, decreasing the efficiency, especially at lower current densities. This results in an overall energy efficiency curve that is not a monotonically increasing function of current density but shows a maximum. Pulsations temporarily increase the current density, which, in this case, improves the efficiency. We stress that this is an important exception that can only occur in bipolar stacks.

2.4. Erroneous comparisons

We emphasise the importance of correctly estimating consumed energy. Ideally, energy consumption should be calculated using Eq. (4) rather than simply multiplying I_{av} and V_{av} as is done in Refs. [24,25]. This is because the time-average of the product of I and V , the instantaneous power, is not in general equal to the product $I_{av}V_{av}$ of their time averages. Therefore, comparing pulsed and DC methods only based on the 'average voltage' or the average current' would not provide a complete understanding of the efficiency or energy consumption of the pulsed method.

Several studies [23,29] look at the 'apparent power' $\frac{1}{T} \sqrt{\int_0^T I^2(t) dt \int_0^T V^2(t) dt}$. However, this is not equal to and by the Cauchy-Schwarz inequality, actually always more than the 'active power' $\frac{1}{T} \int_0^T IV dt$ in the case of pulsating potentials. Ironically, a reference is quoted [30] that warns of the misleading nature of the apparent power.

2.5. Bubble resistance

An instance where a pulsed current could help is when the cell voltage is besides a function of current density, also a function of time. Lowering or switching off the current density could result in a subsequently lowered cell voltage, decreasing the product jV in Eq. (5). This may be relevant in the case of strong mass transfer limitations. Switching off the current allows equilibration of reactants, reducing the concentration overpotentials upon switching back on. However, it was shown numerically [31] that any form of voltage modulation, while leading to higher on-time currents, can never lead to a higher average current than DC. It seems likely that a similar conclusion can be drawn for current modulation.

Another instance of a time dependence of the cell voltage can arise through the effect of bubbles. To see under what conditions this could lead to an improvement due to pulsed potentials, let us study a simplified toy model in which the DC cell voltage can be linearised as $V = V_0 + ARj_{av}$, with A the electrode area and R the cell resistance. Let us assume that during the time t_{off} that the current is off, the resistance approximately returns to its bubble-free value, and during the on-time t_{on} , the resistance is, on average, decreased to $R - \Delta R$. From Eq. (3), an improvement in energy efficiency can be obtained when $\frac{1}{T}j(V_0 + A(R - \Delta R))t_{on} < j_{av}V$. With $T = t_{on} + t_{off}$ and the average current density $j_{av} = \frac{t_{on}}{T}j$, this requires $(R - \Delta R)j < Rj_{av}$ or

$$\frac{t_{off}}{T} < \frac{\Delta R}{R}$$

So, the fraction of the time that the current is switched off should be smaller than the relative decrease in resistance to obtain an improvement in energy consumption compared to DC at equal average current density. As an example, in the zero-gap configuration of Ref. [32] it was obtained that $\Delta R/R \approx 1/4$ and that the bubble resistance arises over a time-scale of the order of 10 s. In case the bubble resistance can be made to disappear in the order of $t_{off} \leq 1$ s, it may be worthwhile to use pulsed potentials with a period of at most a few seconds. Note that the maximum improvement will be a decrease in resistance by about 1/4th. Since there may be additional costs or degradation associated with pulsing, it may be more worthwhile to try to reduce the bubble

overpotential itself.

2.6. Improved kinetics

The pulsing may be hoped to be beneficial for the kinetics. However, whether the lost production during times of lowered or zero current can be made up for by such improvement remains to be investigated.

Finally, no study in the literature shows convincingly that the specific energy consumption can be improved at an equal hydrogen production rate.

3. Experimental methods

Fig. 1 shows the components of our AEM cell with a PiperION® membrane 40 micrometres and 0.6 mm thick Ni-Fe coated stainless steel fibre felt Catrode® anode. Both the electrode and membrane were procured from the Fuel Cell Store. In subsequent sections, this electrode will be referred to as 'Ni/Fe'. In one configuration, we used the same electrode also as the cathode, a configuration we will refer to as Ni/Fe || Ni/Fe, while as an alternative, we changed it for a Pt/C (Tanaka Kikinokoku Singapore Pte. Ltd. TEC10E50E, 46 % Pt) coated carbon paper (CP) with a Pt loading of 0.2 mg/cm² electrode, which we will refer to as Ni/Fe || Pt/C. This cathode from has a Pt loading of 0.2 mg/cm². The active electrode area was 10 cm². A SS316 current collector with an engraved serpentine flow field and an EPDM gasket was used to ensure uniform compression. All components were assembled and compressed between two 3-cm-thick acrylic plates. All experiments were performed in a 1 M KOH (99.99 % from Sigma-Aldrich) electrolyte solution prepared in deionised (DI) water and were conducted at room temperature (20°C). A 5 V DC solar/DC water pump with a flow rate of 3.3 mL/s was used to circulate the electrolyte from the anode side. A Gamry Reference 3000 with a 30k booster was used for electrochemical measurements. The system provides a voltage resolution of 1 μV with a noise level of 2 <μV rms and a minimum current resolution of 100 nA. The system has a rise time of 250 <ns and a minimum hardware time base of 3.333 μs, while the Booster provides a slew rate of 20 V μs⁻¹ and a unity-gain bandwidth of at least 550 kHz. The sampling interval was adjusted to the pulse frequency (from 10 ms down to 100 μs), and looped acquisition was used for high-frequency measurements to avoid data buffer limitations during 20-min tests. Sampling interval details at each frequency are provided in Table S1. Pulsed and DC performances were tested within a frequency range of 0.009-90.9 Hz for $D = 0.9$, and within 0.005-500 Hz for $D = 0.5$. These frequencies follow a logarithmic decade spacing and ensure that the relevant dynamic response is sampled over several orders of magnitude for each duty condition. To avoid performance drift and ensure comparison against a consistent baseline, DC operation was recorded at the start of each day as well as before and after each pulsed run. Because each measurement was 20 min long and the number of pulsed conditions was large, repetition of every case was not feasible. Nonetheless, several representative pulsed conditions were repeated. For instance, low-amplitude pulses at $D = 0.5$, $f = 0.5$ Hz and $D = 0.9$, $f = 0.9$ Hz, during three independent runs ($n = 3$), showed a relative variation of approximately 2.5-3 % in the SEC ratio. For higher-current conditions ($j = 500$ mA/cm²) with higher-amplitude pulsing, for two repetitions ($n = 2$) at $D = 0.5$, $f = 0.5$ Hz and $D = 0.9$, $f = 0.9$ Hz exhibited variations of approximately 3-5 %. Based on this observed spread, a conservative uniform uncertainty of ± 4 % was adopted.

We used a transparent PMMA end plate, a stainless steel current collector, and a serpentine see-through flow channel, see Fig. 1. The membrane was placed between two square-shaped electrodes, both with a geometric area of 10 cm² in a zero-gap configuration. Before assembling, the membrane was activated using the procedure outlined in Ref. [33]. Before starting the measurements, the electrodes were pre-conditioned by ramping up the current density from $j = 50$ mA/cm²

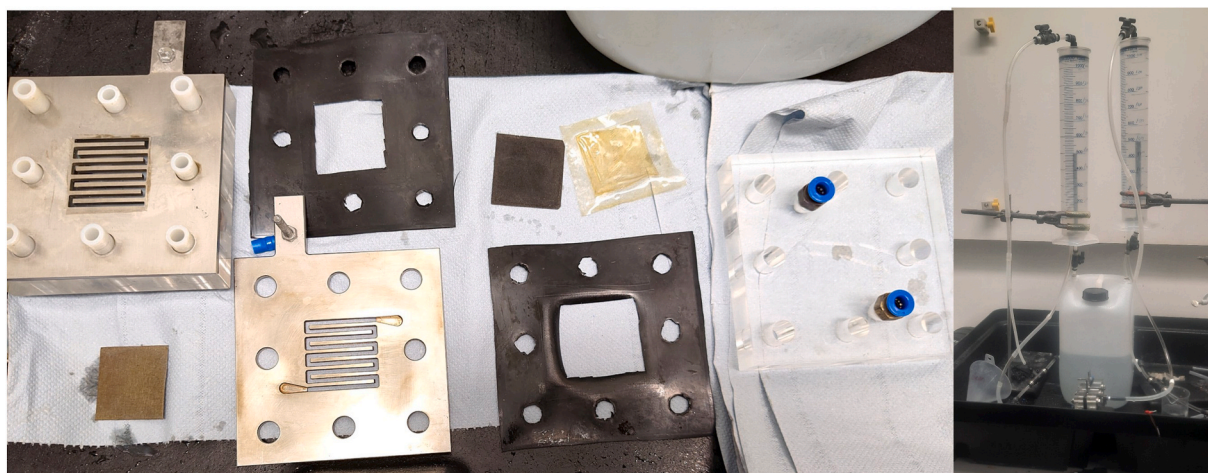


Fig. 1. Images of AEM cell components (left) and complete setup up including AEM cell, water tank, and Faradaic efficiency measurement setup.

through $j = 100 \text{ mA/cm}^2$ to $j = 300 \text{ mA/cm}^2$. Each current density was maintained for 20 min (Fig. S1 and S2) to activate and stabilise the electrodes. After activation for each configuration, the DC chronopotentiometry plot was recorded at constant current density $j_{av} = 295 \text{ mA/cm}^2$ (Fig. S3 and S4). During subsequent measurements, a current was applied in a square waveform with a duty cycle of $D = 0.5$ and, subsequently, 0.9. The peak value of the current pulses was, in these cases, adjusted to $j_{high} = 340 \text{ mA/cm}^2$ and $j_{high} = 300 \text{ mA/cm}^2$, respectively. These higher peak current values compensate for the lower value of $j_{low} = 250 \text{ mA/cm}^2$, in order to maintain the desired average current density of 295 mA/cm^2 . The resulting applied current profiles for $f = 0.5 \text{ Hz}$ and 0.9 Hz are shown in Fig. 2. The rest of the applied current pulses and corresponding voltage profiles are shown in the supplementary information. For computing instantaneous power, the raw current, voltage and time data were processed using MATLAB, where instantaneous power was calculated as the point-wise product of current and voltage $P(t_i) = I(t_i)V(t_i)$. The average power was obtained by numerical integration of $P(t)$ ($P_{avg} = \frac{1}{T} \int_0^T P(t) dt$) over the measurement interval. All integrations were performed on digitised waveforms rather than on instrument-averaged values.

The Faradaic efficiency was determined by measuring the collected hydrogen and oxygen gas volumes. Two calibrated measuring cylinders of 1000 mL volume with divisions of 10 mL were used. Each calibrated cylinder has one inlet for incoming gas, a return water outlet at the bottom, and one gas outlet at the top. The volume of the produced gas was measured by the displacement of the water in the cylinder. The theoretical gas volume was calculated using a molar volume of 24 L/mol for dry gas at ambient pressure and temperature, which closely matches

the experimental conditions. At 20°C , and ambient pressure, a correction of 2.3% is estimated in the FE due to the presence of water vapour. We conservatively estimate the uncertainty in the collected gas volume to be $\pm 5 \text{ mL}$, corresponding to half the smallest graduation of the cylinder and accounting for meniscus reading. For typical collected volumes (440 mL for H_2) this corresponds to an uncertainty of approximately $\pm 1\text{--}2 \%$ in the calculated Faradaic efficiency.

4. Experimental results

4.1. Effect of current pulses on specific energy consumption

In this section, we compare the pulsed current method with DC using the specific energy consumption (SEC) defined in Eq. (4) as the power consumption per H_2 mass produced. For easy comparison, we plot the ratio $\text{SEC}_{\text{pulse}}/\text{SEC}_{\text{DC}}$ of Eq. (5) against frequency f (Hz) while maintaining the average current density $j_{av} = 295 \text{ mA/cm}^2$ equal between the pulsed and DC cases.

The pulsed current profile alternated between 250 and 300 mA/cm^2 when the duty cycle $D = 0.9$ shown in Fig. 2(b) was applied. As seen from Fig. 3 the specific energy consumption ratio $\text{SEC}_{\text{pulse}}/\text{SEC}_{\text{DC}}$ varied between 1 and 1.03 using Ni/Fe at the cathode and between 0.99 and 1 when Pt/C was used as the cathode. This indicates that the pulsed current and DC process exhibit comparable efficiency and energy consumption to produce the same amount of hydrogen. This outcome is perhaps not too surprising given that the peak current of the applied pulse profile with $j_{high} = 300 \text{ mA/cm}^2$ is close to the DC value of 295 mA/cm^2 (see Fig. 2(b)) and the electrolyser was mostly in the ‘on’

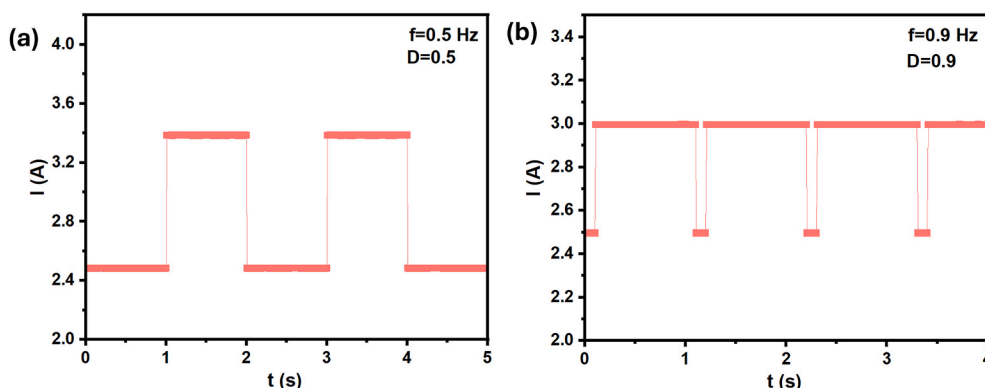


Fig. 2. Applied current pulse profile with (a) $f = 0.5 \text{ Hz}$, $D = 0.5$, (b) $f = 0.9 \text{ Hz}$, $D = 0.9$.

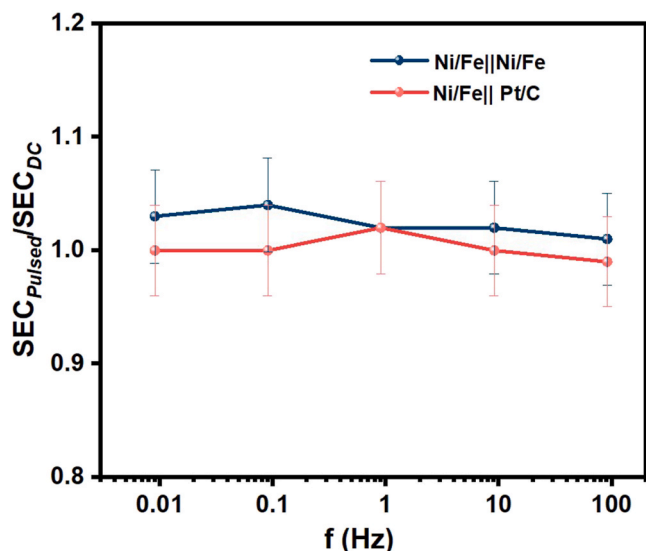


Fig. 3. Plot of SEC ratio against f with $D = 0.9$, using the current profile of Fig. 2(b). The indicated ratio of specific energy consumption (SEC) is defined in Eq. (5). Error bars indicate $\pm 4\%$ conservative experimental uncertainty.

condition rather than ‘off’ state.

We then studied the effect of current pulses with $D = 0.5$. Current pulses fluctuating between 250 mA/cm^2 and 340 mA/cm^2 (shown in Fig. 2(a)) were applied. The plot of the SEC ratio vs f (Fig. 4) shows that the ratio remained above 1 (1.01–1.04) for all frequencies. This slight increase in relative energy consumption, compared to $D = 0.9$ is attributed to the substantially higher ‘on’ current compared to the DC average. This results in higher power consumption during the ‘on’ state while keeping the overall H_2 production is the same, negatively impacting the efficiency of the pulsed method.

4.2. Faradaic efficiency

Across nearly all frequencies and duty cycles, the FE of H_2 remained close to 100 %, as shown in the supporting information (Fig. S5). This shows that almost all of the electrons are used for the hydrogen evolution reaction, as expected. However, a decrease in FE to 93 % and 91 % was observed at 500 Hz for the two configurations, respectively. This

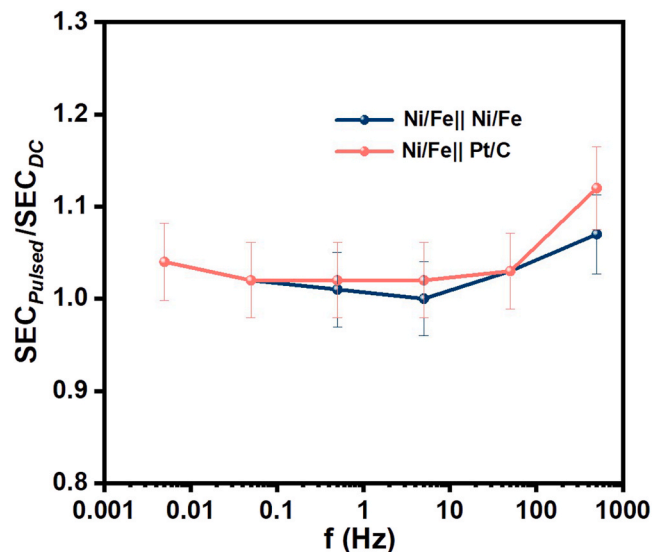


Fig. 4. Plot of SEC ratio against f with $D = 0.5$. Here SEC represents Specific Energy Consumption.

drop we were able to attribute to the potentiostat’s inability to respond quickly enough to the applied pulses, due to capacitive effects, resulting in a deviation from the ideal square wave (Figure S8 (f) and Figure S9 (f)). At 500 Hz with a 50 % duty cycle, the rms deviation of the measured current from the expected square waveform was approximately 4.3 % for the small-amplitude modulation pulse (2.5–3.0 A) and 8.5 % for the high-amplitude pulse. Additionally, for $f = 5000 \text{ Hz}$, the rms deviation increased to 24 % (Fig. S13) and hence was excluded from any SEC analysis in this manuscript. Therefore, we omitted the highest test frequencies from the results shown here.

4.3. Current pulses with high amplitudes

We further investigated higher amplitude current pulses with duty cycles of $D = 0.5, 0.9, 0.99$, as shown in Fig. 5. For these additional experiments, Pt/C was used as the cathode material. For the lower current density, we chose an ‘almost off’ but small non-zero value $j_{\text{low}} = 10 \text{ mA/cm}^2$ to avoid polarity reversal. The value of j_{high} was 580 mA/cm^2 for $D = 0.5$, 327 mA/cm^2 for $D = 0.9$, and 298 mA/cm^2 for $D = 0.99$ to sustain an average current density j_{av} of 295 mA/cm^2 . The rest of the high-amplitude current pulses and corresponding voltage responses are provided in the supplementary information.

As seen in Fig. 6, the specific energy consumption (SEC) for $D = 0.9$ and $D = 0.99$ is again close to or above that of DC, demonstrating no advantage of pulsed current over DC. Notably, for $D = 0.5$, the SEC ratio increased significantly, ranging between 1.3 and 1.7, depending on frequency. Again, this increase results from the higher power consumption during the ‘on’ state, reinforcing the conclusion that reduced D leads to greater power consumption. This contrasts with previous literature because these typically have not attempted to keep the amount of hydrogen produced constant.

Finally, we tested the performance at a higher average current density j_{av} of 500 mA/cm^2 at $D = 0.5$ and $D = 0.9$ with frequencies $f = 0.5 \text{ Hz}$ and 0.9 Hz , respectively. These results, shown in (Fig. S14 and S15), again confirm that DC consistently consumes less energy than pulsed methods.

We can also illustrate these results using the model equations of section 2.2, although this model does not predict any dependence on frequency. The measured DC voltage of about $V = 2.9 \text{ V}$ at $j = 295 \text{ mA/cm}^2$ and 3.6 V at 500 mA/cm^2 (Fig. S16 and S17) may be fitted with a simple offset-resistance model $V \approx V_0 + ARj$ using $V_0 \approx 1.9 \text{ V}$ and $AR \approx 3.4 \Omega \text{ cm}^2$. Note that both values also include some activation losses. For $D = 0.99, 0.9$, and $D = 0.5$ and $j_{\text{low}} \approx 0$, a current $j_{\text{high}} = 298, 328$, and 590 mA/cm^2 was used to obtain the same $j_{\text{av}} = Dj_{\text{high}} = 295 \text{ mA/cm}^2$ as in the case of DC. Inserting these values in Eq. (8) gives $\text{SEC}/\text{SEC DC} \approx 1, 1.04$, and 1.35 for $D = 0.99, 0.9$, and 0.5 , respectively. These values agree roughly with Fig. 6.

5. Conclusions

Through experiments and theoretical reasoning, we proposed what we consider a fair metric to compare pulse and DC methods. While most of the literature compares the time-averaged voltage during current pulsing or the average current during voltage pulses, it does not compare at an equal average hydrogen production rate, which is an important measure. We argued that the pulse method and DC should only be compared in terms of energy efficiency or specific energy consumption for an equal hydrogen production rate. If the current efficiency in pulsed and DC operations is equal, the average current density must be kept equal. We note that our conclusions applied to the single-cell geometry we examined in our study. As noted earlier, bipolar stacks with shunt currents may respond differently to pulsing and should be evaluated separately. We argue and experimentally showed that typically when the average current density is equal, any deviation from DC leads to higher energy consumption. This occurs because the increase in voltage

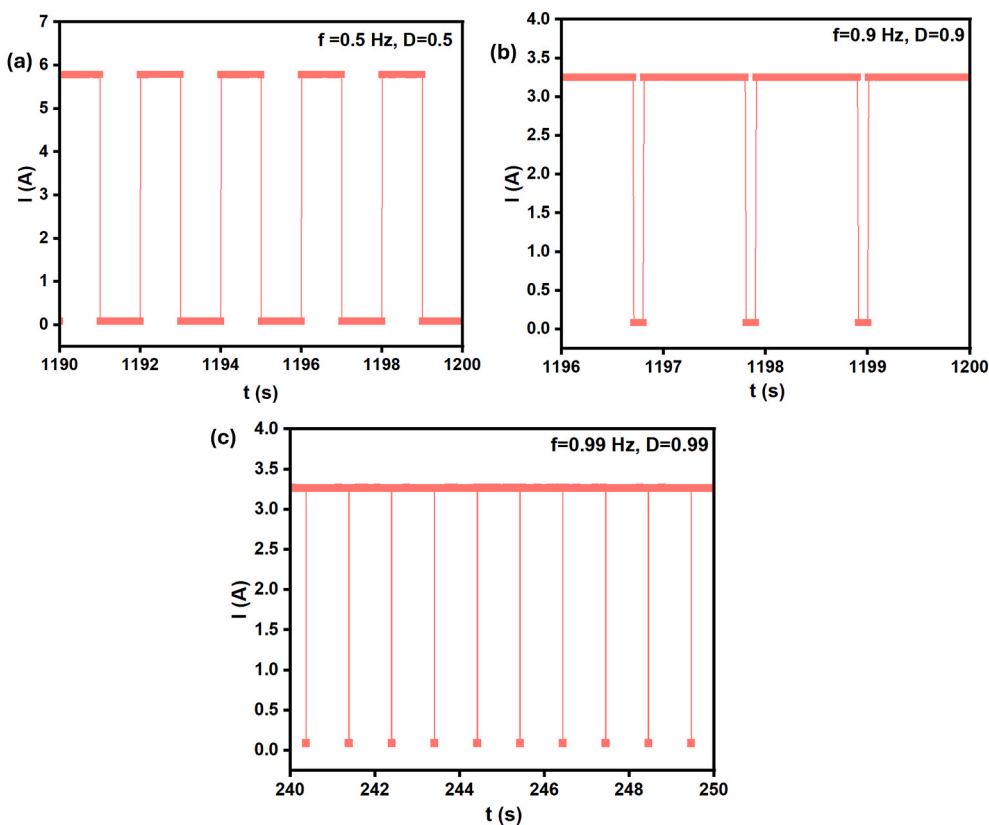


Fig. 5. Current pulses with high amplitudes with D of (a) 0.5, (b) 0.9 and (c) 0.99. In all cases $j_{av} = 295 \text{ mA/cm}^2$ is maintained.

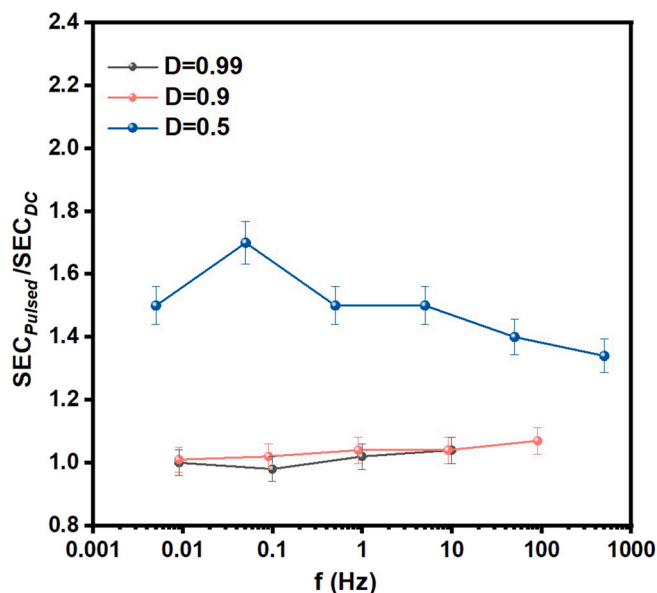


Fig. 6. High amplitude current pulses with close to 'off' lower current density (Fig. 5) and a duty cycle D of (a) 0.5, (b) 0.9 and (c) 0.99. In all cases $j_{av} = 295 \text{ mA/cm}^2$ is maintained. A Ni/Fe anode Pt/C cathode was used in these measurements (Ni/Fe || Pt/C).

during the increased current is usually not fully compensated by the decrease in voltage during the lower current.

Since average current density is an important performance metric in water electrolysis, these findings require a reassessment of the widely perceived benefits of pulsed electrolysis. Future work may extend these investigations to industrially relevant conditions and evaluate promising

dynamic strategies, particularly in scenarios with fluctuating, intermittent power supply, such as photovoltaic or wind energy inputs.

CRediT authorship contribution statement

Anamika Ghosh: Writing – review & editing, Writing – original draft, Visualization, Validation, Methodology, Investigation, Formal analysis, Data curation, Conceptualization. **J.W. Haverkort:** Writing – review & editing, Writing – original draft, Validation, Supervision, Resources, Project administration, Conceptualization.

Declaration of competing interest

The authors declare that they have no known competing financial interests or personal relationships that could have appeared to influence the work reported in this paper.

Acknowledgement

We gratefully acknowledge TNO Petten for providing the PMMA end plate and the flow field-engraved current collector used in this study.

Appendix A. Supplementary data

Supplementary data to this article can be found online at <https://doi.org/10.1016/j.ijhydene.2026.154195>.

References

- [1] Xia F, Li C, Ma C, Li Q, Xing H. Effect of pulse current density on microstructure and wear property of Ni-TiN nanocoatings deposited via pulse electrodeposition. *Appl Surf Sci* 2021;538:148139.
- [2] Lee H, Ren H. Tuning electrocatalytic oxygen reduction reaction with dynamic control of electrochemical interfaces. *J Am Chem Soc* 2024;146:11126–32.

- [3] Casebolt R, Levine K, Suntivich J, Hanrath T. Pulse check: potential opportunities in pulsed electrochemical CO₂ reduction. *Joule* 2021;5:1987–2026.
- [4] Cheng H, Xia Y, Hu Z, Wei W. Optimum pulse electrolysis for efficiency enhancement of hydrogen production by alkaline water electrolyzers. *Appl Energy* 2024;358:122510.
- [5] Tseung ACC, Vassie PR. A study of gas evolution in teflon bonded porous electrodes—iii. Performance of teflon bonded Pt black electrodes for H₂ evolution. *Electrochim Acta* 1976;21:315–8.
- [6] Ghoroghchian J, Jo M B. Use of a homopolar generator in hydrogen production from water. *Int J Hydrogen Energy* 1985;10:101–12.
- [7] Rocha F, de Radiguès Q, Thunis G, Proost J. Pulsed water electrolysis: a review. *Electrochim Acta* 2021;377:138052.
- [8] Liu T, Wang J, Yang X, Gong M. A review of pulse electrolysis for efficient energy conversion and chemical production. *J Energy Chem* 2021;59:69–82.
- [9] Wang Z, Liu Y, Liu S, Cao Y, Qiu S, Deng F. A bibliometric analysis on pulsed electrolysis: electronic effect, double layer effect, and mass transport. *Catalysts* 2023;13:1410.
- [10] Masaud Z, Liu G, Roseng LE, Wang K. Progress on pulsed electrocatalysis for sustainable energy and environmental applications. *Chem Eng J* 2023;145882.
- [11] Živković LA, Kandaswamy S, Petkovska M, Vidaković-Koch T. Evaluation of electrochemical process improvement using the computer-aided nonlinear frequency response method: oxygen reduction reaction in alkaline media. *Front Chem* 2020;8:579869.
- [12] Miličić T, Sivasankaran M, Blümner C, Sorrentino A, Vidaković-Koch T. Pulsed electrolysis—explained. *Faraday Discuss* 2023;246:179–97.
- [13] Hitz C, Lasia A. Determination of the kinetics of the hydrogen evolution reaction by the galvanostatic step technique. *J Electroanal Chem* 2002;532:133–40.
- [14] Shimizu N, Hotta S, Sekiya T, Oda O. A novel method of hydrogen generation by water electrolysis using an ultra-short-pulse power supply. *J Appl Electrochem* 2006;36:419–23.
- [15] Mazloomi K, Sulaiman NB, Moayedi H. An investigation into the electrical impedance of water electrolysis cells—with a view to saving energy. *Int J Electrochem Sci* 2012;7:3466–81.
- [16] Huang C. Solar hydrogen production via pulse electrolysis of aqueous ammonium sulfite solution. *Sol Energy* 2013;91:394–401.
- [17] Lin M-Y, Hourng L-W. Effects of magnetic field and pulse potential on hydrogen production via water electrolysis. *Int J Energy Res* 2014;38:106–16.
- [18] Dobó Z, Palotás ÁB. Impact of the current fluctuation on the efficiency of alkaline water electrolysis. *Int J Hydrogen Energy* 2017;42:5649–56.
- [19] Dobó Z, Palotás ÁB. Impact of the voltage fluctuation of the power supply on the efficiency of alkaline water electrolysis. *Int J Hydrogen Energy* 2016;41:11849–56.
- [20] Vincent I, Choi B, Nakoji M, Ishizuka M, Tsutsumi K, Tsutsumi A. Pulsed current water splitting electrochemical cycle for hydrogen production. *Int J Hydrogen Energy* 2018;43:10240–8.
- [21] De Radigues Q, Thunis G, Proost J. On the use of 3-D electrodes and pulsed voltage for the process intensification of alkaline water electrolysis. *Int J Hydrogen Energy* 2019;44:29432–40.
- [22] Rocha F, Proost J. Discriminating between the effect of pulse width and duty cycle on the hydrogen generation performance of 3-D electrodes during pulsed water electrolysis. *Int J Hydrogen Energy* 2021;46:28925–35.
- [23] Ereli NC, Kst M, Eşiyok T, Özdoğan E, Hüner B, Demir N, et al. First pulsed control system design for enhanced hydrogen production performance in proton exchange membrane water electrolyzers. *Fuel* 2024;371:132027.
- [24] Zhang X, Zhou W, Huang Y, Xie L, Li T, Kang H, et al. Pulsed dynamic electrolysis enhanced PEMWE hydrogen production: revealing the effects of pulsed electric fields on protons mass transport and hydrogen bubble escape. *J Energy Chem* 2025;100:201–14.
- [25] Zhang S, Cao X, Wang B, Wei J, Zhou L, Han J, et al. Application of high-frequency pulsed electrolysis technology in enhancing hydrogen production efficiency and energy saving potential analysis. *Int J Hydrogen Energy* 2025;109:684–93.
- [26] Zhang X, Zhou W, Huang Y, Ding Y, Li J, Xie L, et al. Enhanced hydrogen production enabled by pulsed potential coupled sulfite electrooxidation water electrolysis system. *Renew Energy* 2024;227:120464.
- [27] Wei C, Xu ZJ. The possible implications of magnetic field effect on understanding the reactant of water splitting. *Chin J Catal* 2022;43:148–57.
- [28] Puranen P, Ruuskanen V, Järvinen L, Niemelä M, Kosonen A, Kauranen P, et al. Calculating active power for water electrolyzers in dynamic operation: simple, isn't it? *Int J Hydrogen Energy* 2024;91:267–71.
- [29] Demir N, Kaya MF, Albawabiji MS. Effect of pulse potential on alkaline water electrolysis performance. *Int J Hydrogen Energy* 2018;43:17013–20.
- [30] Filipski PS. Apparent power—a misleading quantity in the non-sinusoidal power theory: are all non-sinusoidal power theories doomed to fail? *Eur Trans Electr Power* 1993;3:21–6.
- [31] Viswanathan K, Cheh HY, Standart GL. Electrolysis by intermittent potential. *J Appl Electrochem* 1980;10:37–41.
- [32] Haverkort JW, Rajaei H. Voltage losses in zero-gap alkaline water electrolysis. *J Power Sources* 2021;497:229864.
- [33] **PiperION® Anion Exchange Membrane, 40 microns, Self-Supporting.**
- [34] Shaaban AH. Water electrolysis and pulsed direct current. *J Electrochem Soc* 1993; 140:2863.
- [35] Speckmann F-W, Bintz S, Groninger ML, Birke KP. Alkaline electrolysis with overpotential-reducing current profiles. *J Electrochem Soc* 2018;165:F456.
- [36] Paulec T, Tvarozek J, Simko J, Prazenica M, Spanik P, Šedo J, et al. Introduction to the issue of the use of voltage and current pulses in the electrolytic production of hydrogen. In: 2024 ELEKTRO (ELEKTRO); 2024. p. 1–6.